Journal of Controlled Release 256 (2017) 68–78

Contents lists available at ScienceDirect

Journal of Controlled Release

journal homepage: www.elsevier.com/locate/jconrel

Membrane permeation of arginine-rich cell-penetrating peptides independent of transmembrane potential as a function of lipid composition and membrane fluidity

Rike Wallbrecher[a], Tobias Ackels[b,1], R. Alis Olea[a], Marco J. Klein[c], Lucie Caillon[c], Jürgen Schiller[d], Petra H. Bovée-Geurts[a], Toin H. van Kuppevelt[a], Anne S. Ulrich[c,e], Marc Spehr[b], Merel J.W. Adjobo-Hermans[a], Roland Brock[a,*]

[a] Department of Biochemistry, Radboud Institute for Molecular Life Sciences, Radboud University Medical Center, Geert Grooteplein 28, 6525 GA Nijmegen, The Netherlands
[b] Department of Chemosensation, Institute for Biology II, RWTH Aachen University, 52074 Aachen, Germany
[c] Institute of Biological Interfaces (IBG-2), Karlsruhe Institute of Technology (KIT), POB 3640, 76021 Karlsruhe, Germany
[d] Medical Department, University of Leipzig, Institute of Medical Physics and Biophysics, Härtelstraße 16 – 18, 04107 Leipzig, Germany
[e] Institute of Organic Chemistry, KIT, Fritz-Haber-Weg 6, 76131 Karlsruhe, Germany

ARTICLE INFO

Keywords:
Cell-penetrating peptides
Membrane potential
Lipid composition
Drug delivery
Ceramide
Sphingomyelin

ABSTRACT

Cell-penetrating peptides (CPPs) are prominent delivery vehicles to confer cellular entry of (bio-) macromolecules. Internalization efficiency and uptake mechanism depend, next to the type of CPP and cargo, also on cell type. Direct penetration of the plasma membrane is the preferred route of entry as this circumvents endolysosomal sequestration. However, the molecular parameters underlying this import mechanism are still poorly defined. Here, we make use of the frequently used HeLa and HEK cell lines to address the role of lipid composition and membrane potential. In HeLa cells, at low concentrations, the CPP nona-arginine (R9) enters cells by endocytosis. Direct membrane penetration occurs only at high peptide concentrations through a mechanism involving activation of sphingomyelinase which converts sphingomyelin into ceramide. In HEK cells, by comparison, R9 enters the cytoplasm through direct membrane permeation already at low concentrations. This direct permeation is strongly reduced at room temperature and upon cholesterol depletion, indicating a complex dependence on membrane fluidity and microdomain organisation. Lipidomic analyses show that in comparison to HeLa cells HEK cells have an endogenously low sphingomyelin content. Interestingly, direct permeation in HEK cells and also in HeLa cells treated with exogenous sphingomyelinase is independent of membrane potential. Membrane potential is only required for induction of sphingomyelinase-dependent uptake which is then associated with a strong hyperpolarization of membrane potential as shown by whole-cell patch clamp recordings. Next to providing new insights into the interplay of membrane composition and direct permeation, these results also refute the long-standing paradigm that transmembrane potential is a driving force for CPP uptake.

1. Introduction

Cell-penetrating peptides (CPPs) are emerging drug delivery vehicles because of their capacity to induce efficient cellular uptake of molecules that otherwise do not enter cells [1]. In order to enable a rational optimization of CPPs and understand cell type preference, CPP entry mechanisms have been intensely investigated. The mode of entry depends on peptide concentration, cell type and the conjugated cargo [2–5] but also on structural characteristics of the peptide such as amino acid charge and stereochemistry [6]. At low micromolar concentrations, arginine-rich CPPs are mainly endocytosed, whereas rapid cytoplasmic entry can occur at high concentrations [7]. This entry is associated with the accumulation of peptide at certain membrane areas, called nucleation zones (NZ), which are colocalizing with ceramide platforms [8–10]. Uptake via NZ is restricted to arginine-rich CPPs such as nona-arginine [8], with the human lactoferrin-derived CPP being a

* Corresponding author at: Department of Biochemistry (286), Radboud Institute for Molecular Life Sciences, Radboud University Medical Center, Geert Grooteplein 28, 6525 GA Nijmegen, The Netherlands.
E-mail address: roland.brock@radboudumc.nl (R. Brock).
[1] Current address: Neurophysiology of Behaviour Laboratory, The Francis Crick Institute, London, UK.

http://dx.doi.org/10.1016/j.jconrel.2017.04.013
Received 9 April 2017; Accepted 10 April 2017
Available online 12 April 2017

remarkable exception as this peptide only has four arginine residues [11].

Although the mechanism of CPP internalization has been described to be cell line-dependent, the reasons for these differences are unknown [4]. A considerable amount of research has been conducted on the role of glycosaminoglycans (GAGs) in endocytosis since these are the first (negatively) charged molecules that cationic CPPs encounter when approaching a cell [12,13]. Several studies demonstrated a positive effect of GAGs on CPP internalization [8,14–16]. However, the role of GAGs depends on the type of CPP, and GAGs are probably not acting as autonomous receptors but rather as coreceptors as reviewed by Favretto et al. [13]. This hypothesis is further supported by the finding that in the absence of GAGs, CPPs still bind to the cells and are internalized [17]. Furthermore, the membrane potential (V_{mem}) has been considered a driving force for the internalization of cationic CPPs [18,19].

In direct comparisons of the frequently used cell lines HEK and HeLa we had observed that HEK cells showed a direct cytoplasmic peptide uptake at concentrations at which HeLa cells only showed endocytosis [20,21]. In this study, we made use of these earlier observations to elucidate the molecular and cellular characteristics underlying the difference in uptake mechanisms between these cell lines with regard to the occurrence of direct translocation at low peptide concentrations and nucleation zone-dependent uptake.

Using electrophysiological recordings in living cells during peptide internalization we show that both cell lines differ fundamentally in their membrane characteristics. In HEK cells, direct membrane translocation was independent of membrane potential. By contrast, an intact resting membrane potential was required for the induction of nucleation zones in HeLa cells and, remarkably, this process was associated with a sudden hyperpolarization of the plasma membrane. Lipidomics revealed that, in contrast to HeLa cells, membranes of HEK cells have a low sphingomyelin content, and conversion of sphingomyelin into ceramide further enhances membrane translocation. A role of membrane fluidity and membrane microdomain organisation was established by demonstrating that in HEK cells direct permeation is abolished at room temperature and upon cholesterol depletion. These results also resolve a long-standing dispute according to which fluorescent labelling is incompatible with direct membrane permeation [22], and shall open new directions of research into the interdependence of membrane composition and permeation of macromolecules.

2. Materials and methods

2.1. Materials

Unless stated otherwise, all compounds were obtained from Sigma-Aldrich and cell culture materials from Invitrogen. The used sphingomyelinase (bSMase) is derived from *Bacillus cereus* and provided at a concentration of 138 U/mL. Stock solutions of valinomycin (9 mM) and gramicidin A (1.06 mM) were prepared in DMSO and ethanol, respectively.

2.2. Cell culture

HeLa and HEK293T cells were obtained from the DSMZ (German Collection of Microorganisms and Cell Cultures, Braunschweig, Germany). HeLa cells were cultured in RPMI supplemented with 10% fetal calf serum (FCS) whereas HEK cells were maintained in high glucose DMEM containing 10% FCS. Both cell lines were cultivated in an incubator at 37 °C with 5% CO_2. Cell culture media were purchased from Invitrogen.

2.3. Peptides

For translocation experiments in large unilamellar vesicles, peptides were synthesized on an automated Syro II multiple peptide synthesizer (MultiSynTech, Witten, Germany), using standard solid phase Fmoc protocols. Peptide synthesis reagents, Fmoc-protected amino acids, and 7-(9-Fluorenylmethyloxycarbonylamino)-coumarin-4-acetic acid (Fmoc-ACA-OH) were purchased from Merck Biosciences (Darmstadt, Germany) and/or Iris Biotech (Marktredwitz, Germany). Solvents for peptide synthesis were purchased from Merck (Darmstadt, Germany) or from Biosolve (Valkenswaard, Netherlands), and solvents for HPLC purification were obtained from Fischer Scientific (Geel, Belgium). The C-terminal phenylalanine of each peptide sequence carried a 7-amino-4-methylcarbamoylcoumarin (ACC) moiety that experiences a wavelength shift upon chymotrypsin cleavage. ACC-resin synthesis was performed manually prior to the peptide synthesis [23]. The crude peptides were purified using a high-pressure liquid chromatography (HPLC) device from JASCO (Groß-Umstadt, Germany) on a preparative Vydac C18 column, using a water/acetonitrile gradient supplemented with 5 mM HCl. The purified peptides were characterized by using analytical HPLC (Agilent; Waldbron, Germany) coupled to an ESI mass spectrometer (μTOF Bruker, Bremen, Germany), and were found to be > 95% pure.

Fluorescently labelled peptides were purchased from EMC microcollections (Tübingen, Germany). All peptides were C-terminally amidated and N-terminally labelled with 5,6-carboxyfluorescein or Alexa 488. Peptide concentrations were determined based on the absorbance of fluorescein at 492 nm with a Novaspec II spectrophotometer (Pharmacia, New York, USA). Fluorescein-labelled peptides were diluted in Tris-HCl buffer (10 mM, pH 8.8) and an extinction coefficient of 75,000 M^{-1} cm^{-1} was assumed for calculating peptide concentrations, the Alex488-labelled peptide was diluted into deionized water and extinction measured at 495 nm assuming an extinction coefficient of 73,000 M^{-1} cm^{-1}.

2.4. Confocal laser scanning microscopy

Two days before the experiment 20,000 HeLa cells or 25,000 HEK cells were seeded in chambered coverslips (Nunc, Wiesbaden, Germany or Ibidi, Martinsried, Germany, respectively). Confocal microscopy was performed using a Leica SP5 microscope with an HCX PL APO 63 × N.A. 1.2 water immersion lens (Leica, Mannheim, Germany). During image acquisition, cells were maintained at 37 °C. Fluorescein was excited using an argon ion laser at 488 nm and emission was collected between 500 and 550 nm. Cells were incubated with the indicated peptide concentrations and the specific compounds, as indicated for each experiment. During imaging, cells were maintained in RPMI without phenol red in the presence or absence of 10% FCS.

2.5. Flow cytometry

80,000 HeLa cells or 100,000 HEK cells were seeded in 24-well plates one day before the experiment. After incubating cells for 10 min either with 1 μM gramicidin A or 10 μM valinomycin in RPMI or RPMI alone, cells were co-incubated for 20 min with the indicated peptide concentrations. Cells were washed with RPMI twice, trypsinized, centrifuged and resuspended in RPMI + 10% FCS without phenol red. Fluorescence intensities were measured using a flow cytometer (BD Biosciences, Erembodegem, Belgium). Approximately 10,000 intact cells were gated based on forward and sideward scatter. The Summit 4.3 software (Dako, Fort Collins, USA) was used for the analysis of gated cells.

2.6. Patch-clamp combined with confocal laser scanning microscopy

For electrophysiological recordings, HEK293T cells or HeLa cells were cultured on 35 mm glass dishes and transferred to a recording chamber (Luigs & Neumann, Ratingen, Germany) on an upright fixed-stage scanning confocal microscope (TCS SP5 DM6000CFS, Leica Microsystems, Mannheim, Germany) equipped with an HCX APO L 20 × NA 1.0 water immersion objective (Leica Microsystems) as well as

a cooled CCD-camera (DFC360FX, Leica Microsystems). Fluorescein was excited using the 488 nm line of an argon ion laser. Changes in cytosolic fluorescence were monitored over time at 0.25–1 Hz frame rates. Patch pipettes (4–7 MΩ) were pulled from borosilicate glass capillaries (1.50 mm OD / 0.86 mm ID; Science Products, Hofheim, Germany) on a PC-10 micropipette puller (Narishige Instruments, Tokyo, Japan), fire-polished (MF-830 Microforge; Narishige Instruments) and filled with pipette solution containing 143 mM KCl, 2 mM KOH, 1 mM EGTA, 0.3 mM $CaCl_2$ (free Ca^{2+} = 110 nM), 10 mM HEPES, 2 mM MgATP, 1 mM NaGTP; pH = 7.1 (adjusted with KOH); osmolarity = 290 mOsm. An agar bridge (150 mM KCl) connected the reference electrode and the bath solution. An EPC-10 amplifier controlled by Patchmaster 2.67 software (HEKA Elektronik, Lambrecht, Germany) was used for data acquisition. Both pipette (C_{fast}) and cell membrane capacitance (C_{slow}) were monitored and automatically compensated throughout the experiment. If not stated otherwise, signals were low-pass filtered (analog 3- and 4-pole Bessel filters (−3 dB); adjusted to 1/3–1/5 of the sampling rate (5–10 kHz, depending on protocol)). Electric noise was suppressed using a Hum Bug Noise Eliminator (Quest Scientific, Vancouver, Canada). Between recordings, the holding potential (V_{hold}) was −60 mV. All electrophysiological data were recorded in whole-cell configuration at room temperature. Free Ca^{2+} and Mg^{2+} concentrations were calculated using WEBMAXC STANDARD (available at http://www.stanford.edu/~cpatton/webmaxcS.htm). Cells were continuously superfused with extracellular solution containing 145 mM NaCl, 5 mM KCl, 1 mM $CaCl_2$, 1 mM $MgCl_2$, 10 mM HEPES; pH = 7.3 (adjusted with NaOH); osmolarity = 300 mOsm (adjusted with glucose). Stimuli were applied from air pressure-driven reservoirs via an 8-in-1 multi-barrel 'perfusion pencil' (Science Products, Hofheim, Germany) [24]. Individual numbers of cells / experiments (n) are denoted in the figure legends. If not stated otherwise, results are presented as means ± SEM and statistical analyses were performed using paired or unpaired *t*-tests (as dictated by experimental design). Electrophysiological data were analyzed offline using Patchmaster 2.67 (HEKA Elektronik), IGOR Pro 6.31 (WaveMetrics, Lake Oswego, OR) and Excel (Microsoft, Seattle, WA) software.

2.7. Plasma membrane isolation and lipid analysis

The protocol for extraction of lipids from the plasma membrane was adjusted from Yao et al. [25]. One million cells were seeded in petri dishes (145 mm) and grown for four days. Cells were washed twice with ice-cold HBS + (10 mM HEPES, 135 mM NaCl, 5 mM KCl, 1 mM $MgCl_2$, 1.8 mM $CaCl_2$, pH 7.4, containing protease inhibitor cocktail (Roche, Basel Switzerland) and 1 mM phenylmethylsulfonyl fluoride (Sigma-Aldrich, St. Louis, USA)) and scraped into HBS +. Cells from three petri dishes were pooled and homogenized with an Ultra Turrax (IKA T10 basic, IKA-Werke, Staufen, Germany) 3 times for 5 s with 1 min pause. A Bradford assay (Biorad, München, Germany) was performed to normalize for the protein content of the samples.

Cell lysates were centrifuged at 10,000 × *g* for 45 min at 4 °C using an ultracentrifuge (Sorvall WX80, Thermo Scientific, Waltham, USA). This ultracentrifuge was also used for all subsequent centrifugation steps at 4 °C. Membrane pellets were resuspended in 5% sucrose (in HBS +). Sample volumes corresponding to the same protein amounts were loaded onto a sucrose gradient (45%–20%–5%) and centrifuged overnight at 150,000 × g at 4 °C in a swing-out rotor. The plasma membrane fraction, which was located on top of the 45% and inside the 20% layer, was diluted with HBS + and centrifuged for 30 min at 200,000 × *g*. After resuspending the pellet in 5% sucrose, it was loaded again onto a sucrose gradient and centrifuged for 1 h at 200,000 × *g* using a swing-out rotor. The plasma membrane fraction was collected at the interface of the 45% and 20% layers. The pellet was diluted with milliQ, pelleted at 200,000 × *g* for 30 min and resuspended in 200 μL milliQ for lipid extraction. The lipid extraction (chloroform/methanol) and analysis (by matrix-assisted laser desorption and ionization time-of-flight mass spectrometry) were performed according to Dinkla et al. [26].

2.8. Uptake in large unilamellar vesicles

The lipids 1-palmitoyl-2-oleoyl-*sn*-glycero-3-phosphatidylcholine (POPC), 1-palmitoyl-2-oleoyl-*sn*-glycero-3-phosphatidylglycerol (POPG), cholesterol (CHOL), sphingomyelin (SM, from chicken egg), and 1,2-dioleoyl-*sn*-glycero-3-phosphoethanolamine-*N*-(lissamine rhodamine B sulfonyl) (Rhod-PE) were obtained from Avanti Polar Lipids (Alabaster, USA).

The translocation experiments were based on a modified experimental design according to [27], using a 10 mM PIPES-Na_2 buffer (pH 7.0) containing 10 mg/mL chymotrypsin and 150 mM NaCl. Liposomes were prepared by dissolving the dry lipids (POPC/POPG/CHOL at a molar ratio of 5.5/4.5/1, or POPC/POPG/CHOL/SM at 4.5/4.5/1/1) together with 2–3 μL of rhodamine-PE in MeOH/$CHCl_3$ (1/1 (v/v)). The mixture was dried under a flow of N_2 and placed under high vacuum overnight to remove residual solvent. The obtained thin layer was then re-suspended in the chymotrypsin-containing buffer by vortexing, followed by 10 freeze-thaw cycles using warm water (50 °C) to form multilamellar liposomes. A uniform population of large unilamellar vesicles (LUVs) was obtained by repeated high pressure extrusion of the liposomes through a polycarbonate Unipore membrane (pore size, 100 nm; Millipore) at a temperature above the gel-to-liquid crystal phase transition (POPC/POPG at 2 °C). To remove unencapsulated dye, the vesicles were purified before the experiment by gel filtration on a Sephacryl 500-HR (Sigma-Aldrich, St. Louis, MO) column using a 10 mM PIPES-Na_2/150 mM NaCl elution buffer, which balances the internal vesicle osmolarity. Samples of the vesicles were taken before and after the purification to determine the lipid concentration by spectroscopically determining the amount of rhodamine-PE (ex/em: 540 nm/580 nm, 5 nm slit).

The translocation of the peptides into the vesicles was quantitatively monitored over time from the fluorescence of cleaved ACC that appeared only after contact of the peptides with the chymotrypsin present inside the vesicles. Fluorescence measurements were performed in a thermostated cuvette under constant stirring at 30 °C (i.e. above the transition temperature of all lipids used) in 10 mM PIPES-Na_2 (pH 7.0) containing 150 mM NaCl on a FluoroMax2 spectrofluorimeter (2 nm slit), using the spectroscopic parameters of free ACC (ex/em: 365 nm/470 nm). The peptide was added to the cuvette containing the vesicles after an incubation time of 100 s. The peptide concentration of the final sample was 1 μM with a peptide-to-lipid molar ratio (P/L) of 1:50. The translocation rate of the peptides was determined relative to the translocation rate of the highly membrane permeant chymotrypsin substrate TP1 (PLILLRLLRGQF-ACC) [27] that was set to 100%. Data were acquired in the first 120 s after addition of the peptide to the vesicles.

3. Results

3.1. Differential uptake routes in HeLa and in HEK cells

So far, direct membrane permeation of CPPs has primarily been associated with cargo size and type of CPP [28]. Even though also a cell type-dependence has been reported there is little understanding of the cellular and molecular characteristics underlying these differences. HeLa and HEK cells are commonly used cell lines in in vitro uptake studies, due to their ease of handling and the large body of available data relating to these cells. We had observed before that HEK cells permit direct penetration of the prototypic arginine-rich CPP R9 independent of concentration [20]. To compare HeLa and HEK cells side-by-side, cells were incubated with fluorescein-labelled R9 at different concentrations. In HeLa cells, at low micromolar concentrations uptake occurred by endocytosis (Fig. 1A). Only at peptide concentrations exceeding 10 μM, a concentration-dependent switch to

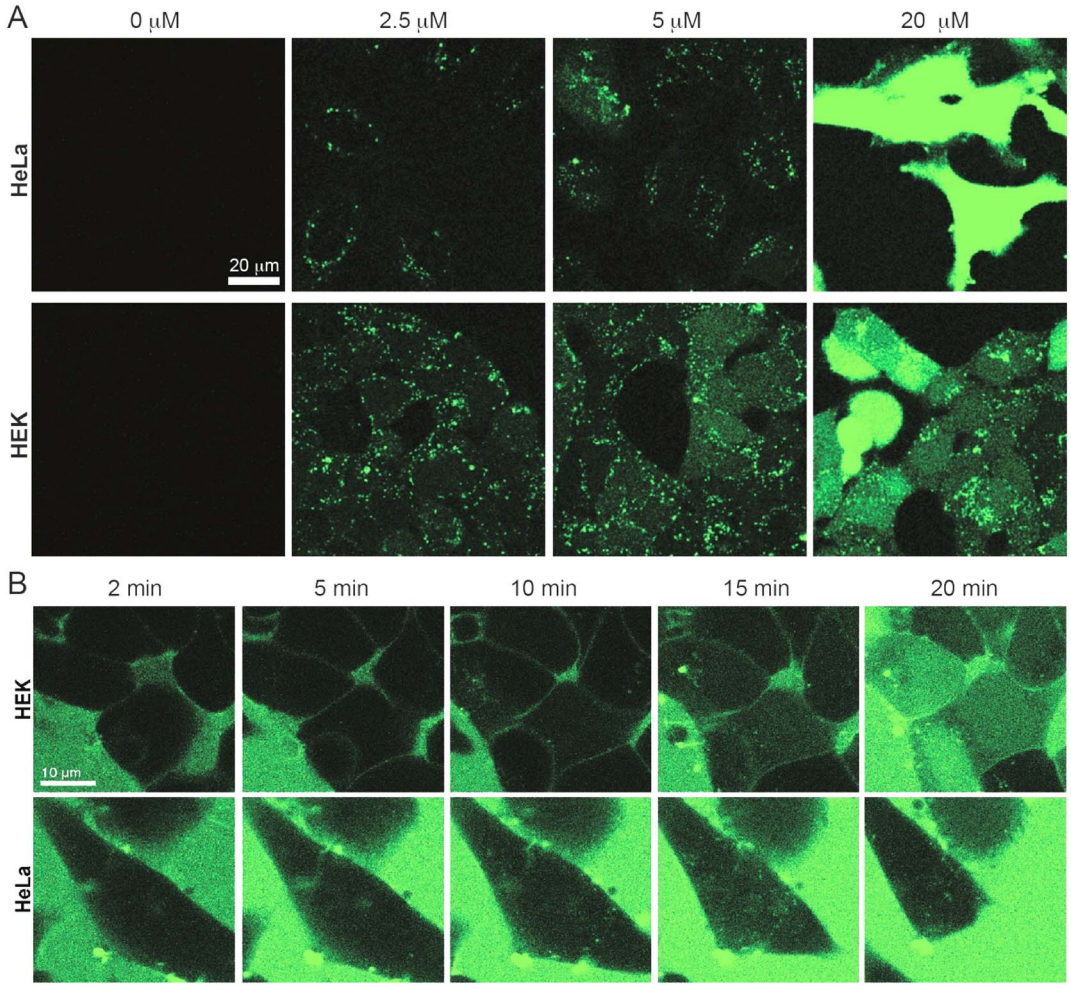

Fig. 1. Differential uptake routes of nona-arginine (R9) in HeLa and HEK cells. (A) Cells were incubated with the indicated concentrations of R9 in RPMI + 10% FCS for 20 min. Cells were washed and imaged by confocal microscopy. (B) Cells were incubated with 5 μM nona-arginine in RPMI + 10% FCS. Images were acquired by confocal microscopy during incubation. Therefore, also some out-of-focus fluorescence is present. Time points indicate the time after the start of the peptide incubation.

a rapid and very efficient cytoplasmic import was observed. We have shown before that this switch depends on the activation of acid sphingomyelinase and ceramide formation [9]. By contrast, HEK cells showed, independent of peptide concentration, a pronounced cytoplasmic fluorescence and less endocytic vesicles. There was no concentration-dependent switch in import mechanism. When cell-associated fluorescence was quantified by flow cytometry, these differences were reflected by a linear dose dependence of uptake in HEK cells and by a very steep increase in cell-associated fluorescence in HeLa cells (see Fig. 5A, control condition). While cytoplasmic influx into HeLa cells at high peptide concentrations occurs rapidly [8], time-lapse microscopy showed a continuous increase of homogenous cytoplasmic and nuclear fluorescence in HEK cells. In HeLa cells, some punctate fluorescence became visible only after 10 min, consistent with uptake by endocytosis (Fig. 1B). It has frequently been argued that the use of fluorescein as a fluorophore can lead to misinterpretation due to the pH dependence of this fluorophore. In order to rule out that the absence of endocytic vesicles for HEK cells was a consequence of pH or concentration dependent quenching inside endosomes, the subcellular distribution of fluorescein-R9 was compared to the one of Alexa488-R9. For this experiment we used HeLa cells as these showed prominent endocytic uptake. The distribution of punctate fluorescence for both peptides in HeLa cells was indistinguishable, and also the degree of colocalization with the endolysosomal probe lysotracker was the same (Supplemental Fig. 1), thereby validating that fluorescein provides a reliable detection of endolysosomal vesicles at this time point. For Alexa488-R9, in HEK cells, less cytoplasmic fluorescence was present, and in HeLa cells NZ-dependent uptake could only be observed at 20 μM under serum-free conditions, which can be explained by the bulkiness and higher charge of Alexa488 which compromises direct crossing of the plasma membrane. To substantiate that the presence of cytoplasmic fluorescence in HeLa cells at high concentrations was not a function of the fluorophore but of the peptide, cells were incubated with a mixture of 2 μM labelled peptide and 20 μM unlabelled R9. While at 2 μM of Fluo-R9 alone, hardly any fluorescence was presence, cells incubated with the mixture showed a homogenous cytoplasmic fluorescence (Supplemental Fig. 2).

To explore the scope of these differences, we also assessed the uptake for penetratin and the D-amino acid isomer r9. In HeLa cells, penetratin only showed a punctate fluorescence independent of concentration [8], while endocytic uptake for r9 was only half that of R9 (Supplemental Fig. 3) [6]. In HEK cells, for r9 only homogenous cytoplasmic staining with prominent nucleolar fluorescence was present, which is in accordance with earlier observations for this stereoisomer [8,29]. Clearly, direct cytoplasmic entry is chirality independent. For penetratin, next to some punctate fluorescence, also a pronounced cytoplasmic fluorescence was observed.

3.2. Both cell lines show similar glycosaminoglycan profiles

Since glycosaminoglycans (GAGs) and sialic acids were shown to be involved in the internalization of CPPs [13], we were interested to learn whether differences in the amount or profile of glycosaminoglycans

between cell lines may contribute to differences in uptake mechanisms. Therefore, we compared the glycocalyx composition of HeLa and HEK cells using a panel of single chain antibodies with preferences for certain GAGs (Supplemental Fig. 4A). Overall, the glycocalyx composition was similar for HeLa and HEK cells. For some epitopes, especially for chondroitin sulfate, HEK cells showed a lower expression. However, complete removal of the glycocalyx did not change the uptake mechanism of R9 (Supplemental Fig. 4B), indicating that the composition of the glycocalyx is not a key determinant for the uptake mechanism.

3.3. Lipid composition as a determinant for uptake mechanism

Next, we hypothesized that the direct membrane translocation of nona-arginine in HEK cells may also be a consequence of a particular lipid composition of the plasma membrane. To compare their lipid content, plasma membranes of HeLa and HEK cells were isolated by sucrose density centrifugation and lipids were detected using mass spectrometry. Remarkably, while the plasma membrane of HeLa cells was rich in sphingomyelin, hardly any sphingomyelin was detected in the isolates of HEK cells (Fig. 2). When HeLa cells were treated with bSMase, ceramide could be detected, which is in agreement with immunofluorescence staining in a previous study that showed colocalization of NZ with ceramide [9].

3.4. Direct membrane permeation in HEK cells is sensitive to temperature and cholesterol depletion

The results so far indicated that the plasma membrane of HeLa cells is resistant to peptide penetration, and direct uptake can occur only after modulation of membrane composition through sphingomyelin turnover. In contrast, for HEK cells the membrane has an intrinsic permissiveness for entry of R9. Temperature and cholesterol content are key determinants for membrane organisation and fluidity. Therefore, we assessed the impact of lower temperatures on uptake. In comparison to 37 °C, the cytoplasmic fluorescence in HEK cells was strongly decreased at 30 °C. This effect was even more pronounced at room temperature (Fig. 3A). Interestingly, cytoplasmic uptake at room temperature could be partially rescued by incubation of cells with sphingomyelinase (bSMase). In contrast, endocytic uptake for HeLa cells was not affected over this temperature range (Fig. 3B, D).

To determine the impact of the various conditions on endocytosis, cells were co-stained with fluorescently labelled transferrin as a marker for clathrin-dependent endocytosis. Overall, HEK cells showed less uptake of transferrin than HeLa cells. Remarkably, for HEK cells, endocytic uptake even increased at lower temperatures. Similar to the impact of temperature, for HEK cells also cholesterol extraction by cyclodextrin treatment reduced cytoplasmic fluorescence. The reduction was the strongest at 37 °C (Fig. 3C, E).

3.5. Membrane potential changes differ between HeLa and HEK cells

Given its previous implication in peptide uptake [19,30], we next addressed the role of the plasma membrane potential (V_{mem}) for peptide uptake in HEK and HeLa cells. Using a combination of confocal microscopy and single-cell patch-clamp, V_{mem} was recorded during peptide uptake. We performed whole cell recordings, meaning that the membrane patch inside the patch pipette was broken and the potential across the whole plasma membrane was measured. Surprisingly, nucleation zone-dependent uptake in HeLa cells was associated with a strong hyperpolarization (Fig. 4). By comparison, in HEK cells, there were no major changes in V_{mem}, except for a slight depolarization, providing further evidence that in these two cell lines direct cytoplasmic uptake occurs by two fundamentally different mechanisms. Strong hyperpolarization was only observed in HeLa cells that showed nucleation zones, as was confirmed by randomly patching cells and then recording their uptake kinetics. It is important to note that during experiments nucleation zones were also observed in non-patched cells, confirming that peptide influx was not a consequence of membrane damage inflicted by patch-clamping the cell. Since patch-clamp recordings had to be performed in HEPES-buffered solution in the absence of FCS, we used reduced peptide concentrations. Serum is known to reduce the effective peptide concentration due to binding to serum proteins (Supplemental Fig. 5) [3]. The degree of hyperpolarization was variable as is the strength of peptide uptake for NZ-dependent uptake {[8] #355}. Therefore, no statistics can be given.

Next, we wanted to investigate whether changing V_{mem} affected the internalization efficiencies in HeLa and HEK cells. As described earlier, valinomycin and gramicidin A induce hyperpolarization and depolarization, respectively [31–33]. We were able to confirm the effects of

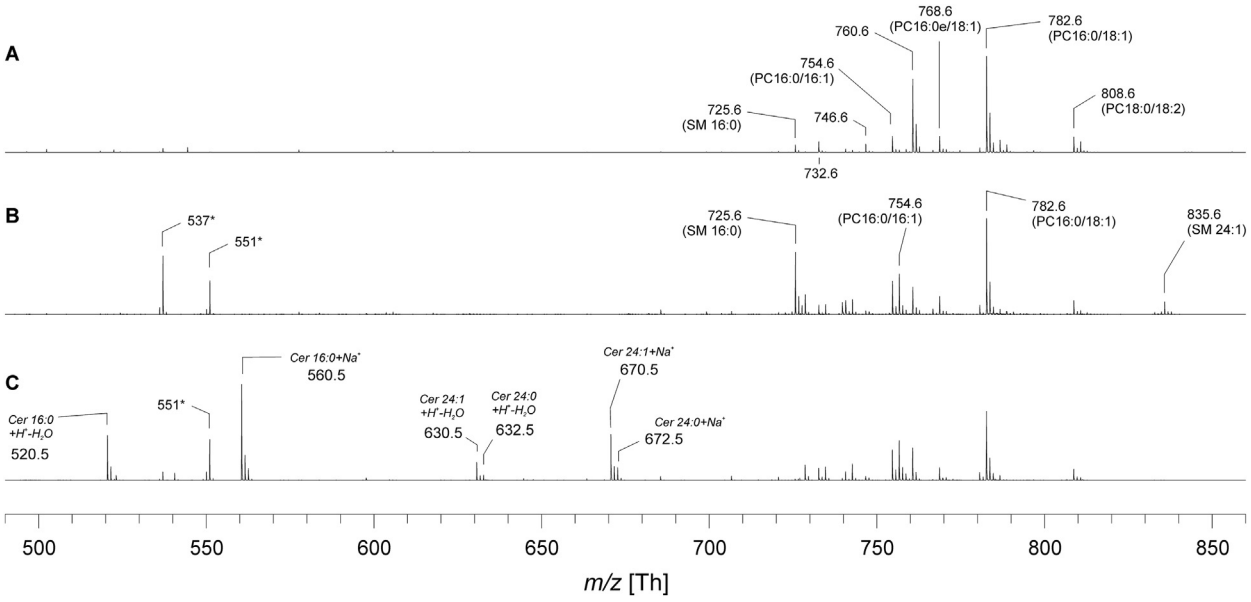

Fig. 2. Positive ion MALDI-TOF mass spectra of membrane lipid extracts from HeLa and HEK cells. Samples were diluted 1:1 (v/v) with the matrix (0.5 M 2,5-dihydroxybenzoic acid in methanol). All peaks are labelled based on their *m/z* ratios and matrix cluster ions are marked by asterisks. (A) HEK cells, (B) HeLa cells, (C) HeLa cells treated for 20 min with 1200 mU/mL bSMase at 37 °C. Cer, ceramide; PC, phosphatidylcholine; SM, sphingomyelin.

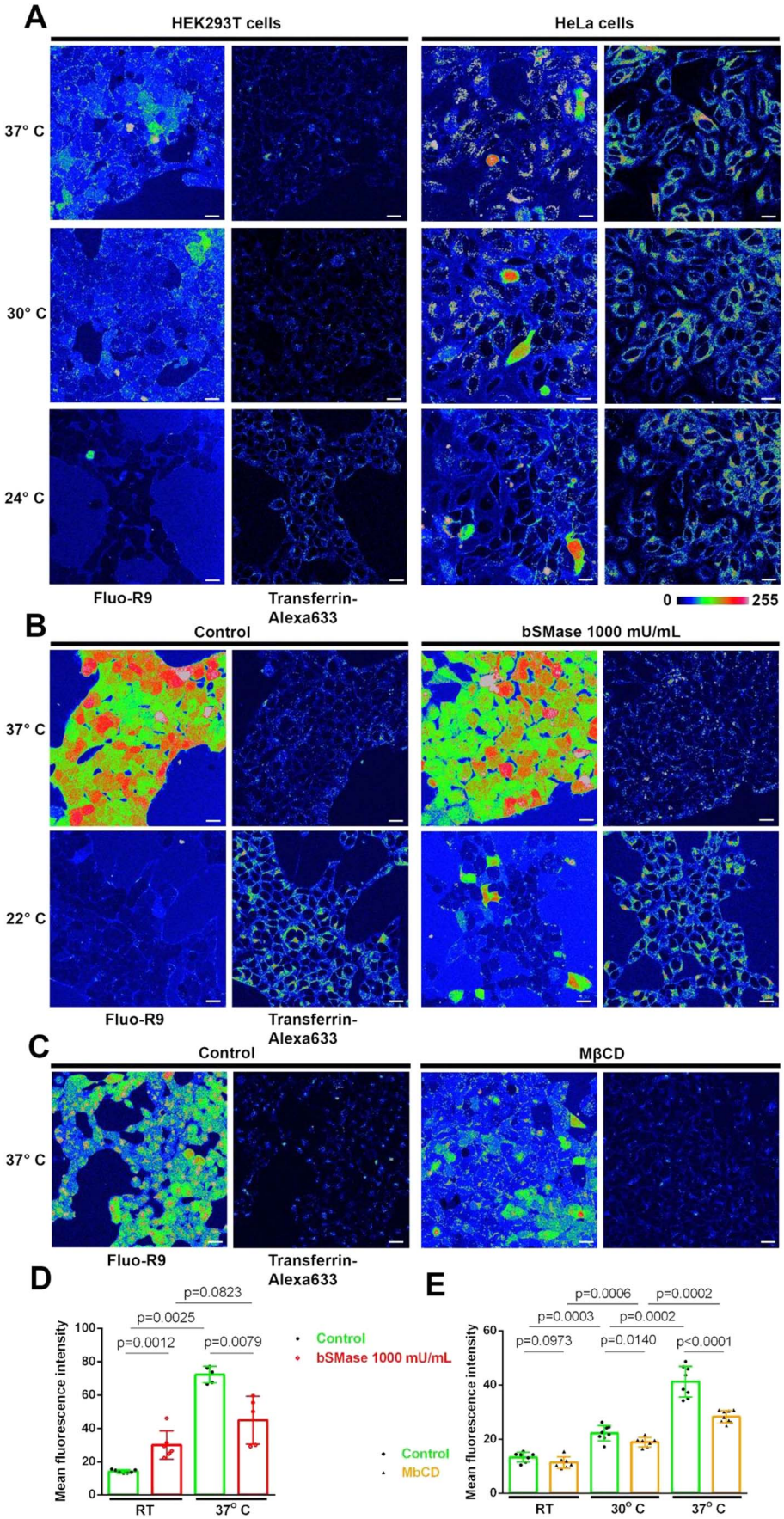

Fig. 3. (A) Direct uptake decreases with temperature. HEK and HeLa cells were treated with 5 μM Fluo-R9 and Transferrin-Alexa633 in the presence of serum for 30 min. (B, D) bSMase partially rescues the Fluo-R9 uptake at room temperature in HEK cells. N = 2; (C, E) Cholesterol extraction with MβCD compromises direct permeation in HEK293T cells. For microscopy, only incubation at 37 °C is shown. Scale bars represent 20 μm. Error bars represent standard deviation.

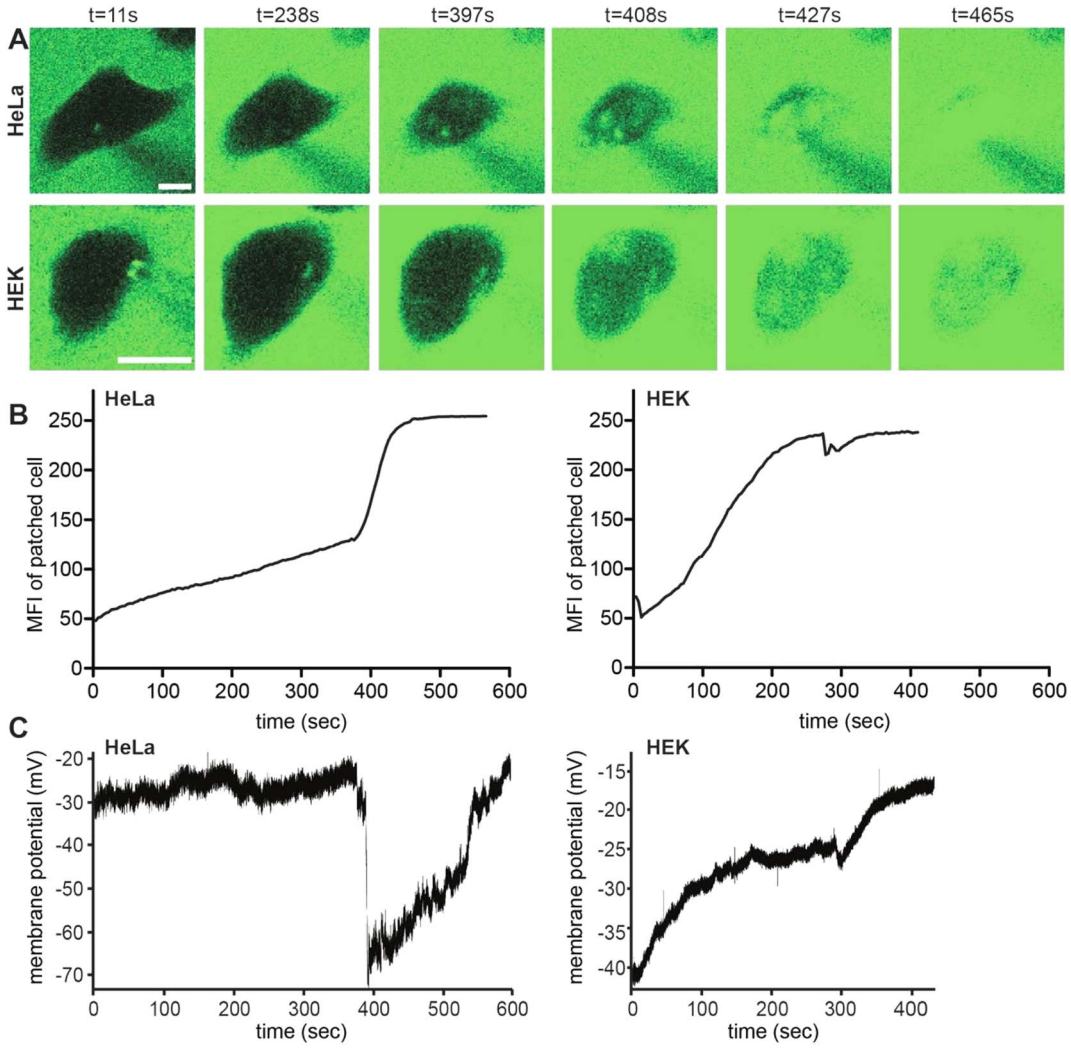

Fig. 4. Membrane potential during R9 internalization in HeLa and HEK cells. (A) Uptake of 10 μM R9 in HEPES buffer into representative patched cells over time. Scale bars denote 10 μm. (B) The mean fluorescent intensities (MFI) of cells (in A) are plotted over time. Note that fluorescence for the patched HeLa cell went into saturation. In this case, confocal microscopy did not intend to provide quantitative information on uptake, but time-resolved data on the onset of NZ-dependent uptake. (C) Membrane potential recordings of the patched cells over time. Graphs in B and C correspond to the cells shown in A. Due to the low numerical aperture of the lens required during patch clamp recordings, images show more out-of-focus fluorescence. Shown is one representative cell for each type of a total of about ten.

both compounds by whole-cell patch-clamp recordings (Supplemental Fig. 6).

At low micromolar concentrations, manipulating V_{mem} did not change the uptake efficiencies in either HeLa or HEK cells. However, depolarizing V_{mem} using gramicidin A dramatically reduced R9 internalization at 10 μM in HeLa cells (Fig. 5). The uptake route was completely shifted from NZ to endocytosis, indicating that NZ-dependent peptide uptake in HeLa cells requires an intact resting membrane potential, whereas endocytotic uptake does not. Hyperpolarization had no significant effect on uptake. By contrast, changing V_{mem} in HEK cells had no major effect on internalization efficiency. The differences in cell-associated intensities between HeLa and HEK cells show that endocytic and, in particular, NZ-dependent uptake in HeLa cells are more efficient than the concentration-independent direct membrane translocation occurring in HEK cells. Interestingly, in HEK cells pre-incubation with gramicidin A even caused a slight increase in uptake efficiency. Thus, the direct peptide translocation in HEK cells is independent of the presence of a transmembrane potential, further underpinning that this translocation is fundamentally different from the NZ-dependent uptake in HeLa cells.

After detecting that the formation of a nucleation zone is accompanied by strong hyperpolarisation, we aimed to further investigate the molecular mechanism of NZ-dependent uptake. Current knowledge regarding molecular uptake mechanisms is sparse except for the involvement of acid sphingomyelinase and subsequent ceramide formation [9]. However, so far the molecular details of events leading to sphingomyelinase activation in general have remained elusive [34]. The possibility to record the membrane potential in parallel to observing peptide uptake allowed us to investigate whether hyperpolarization is a prerequisite for, or a consequence of ceramide formation. We depolarized HeLa cells with gramicidin A, which inhibits NZ-dependent internalization of R9 (Fig. 5), under continuous monitoring of V_{mem} (Fig. 6). Surprisingly, when replacing gramicidin A by bacterial sphingomyelinase (bSMase), we observed rapid cytoplasmic uptake while V_{mem} remained depolarized. These findings show that an intact resting potential is required for triggering sphingomyelinase activation, but once sphingomyelin is converted to ceramide, entry occurs in a potential-independent manner.

3.6. Uptake into large unilamellar vesicles

Considering the prominent role of sphingomyelin in the control of membrane permeation we were interested to learn whether these effects could be recapitulated in large unilamellar vesicles as a

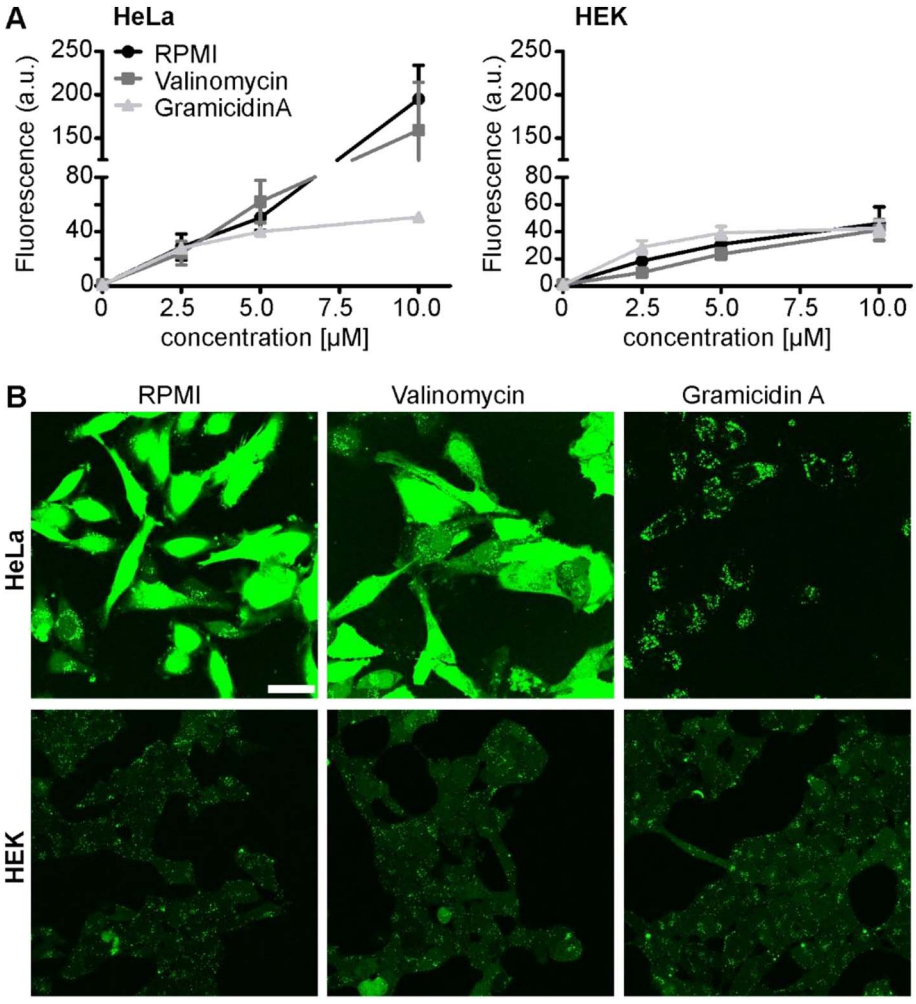

Fig. 5. Impact of membrane potential changes on uptake efficiencies of R9. HeLa and HEK cells were pre-incubated with the indicated compounds or RPMI alone for 10 min which was followed by a 20 min co-incubation with the indicated concentrations of R9. (A) After the incubation, cells were washed, trypsinized and analyzed by flow cytometry. Averages of median fluorescence intensities of three independent experiments are shown. Error bars denote SEM. (B) After incubating with 10 μM R9, cells were washed and imaged using confocal microscopy. Scale bar denotes 40 μm.

minimalistic model system. Using the protocol by Marks et al. [27], uptake was determined into vesicles consisting of a mixture of palmitoyl-oleoyl-phosphatidylcholine (POPC), -glycerol (POPG) and cholesterol, which were prepared with and without sphingomyelin. Initial experiments had shown that the anionic POPG was a prerequisite for the observation of uptake. CPPs were synthesized with a C-terminal aminomethylcarbamoylcoumarin fluorogenic group, linked to the peptide via a chymotrypsin cleavage site. Liposomes were loaded with the protease. Outside the liposomes a protease inhibitor prevented peptide cleavage, in case any enzyme was released from the liposomes as a consequence of membrane disruption. Next to R9 we also included penetratin in our analyses, and we used the highly amphipathic and membrane-active CPP TP1 as an established “gold standard” for this assay [27]. TP1 indeed showed the highest uptake, followed by R9 and penetratin. Interestingly, there was no dependence of uptake on the presence of sphingomyelin (Supplemental Fig. 7).

4. Discussion

In this study we show that direct permeation of R9 through the plasma membrane occurs independent of transmembrane potential. By comparing uptake in HEK and HeLa cells and analyzing their plasma membrane characteristics, we identify sphingomyelin content as an important difference. In HeLa cells, direct cytoplasmic entry requires the conversion of sphingomyelin into ceramide. Once this conversion has occurred, the kinetics and extent of peptide entry exceeds the one for HEK cells. This conversion may either occur through activation of endogenous acid sphingomyelinase at high peptide concentrations or through addition of exogenous sphingomyelinase. Only for the triggering of endogenous sphingomyelinase, an intact resting membrane potential is required.

Direct translocation in HEK cells responds sensitively to a lowering of temperature. Also changes in membrane microdomain organisation through cholesterol extraction abolish direct translocation. These data also underline that cytoplasmic fluorescence results from direct membrane permeation and does not reflect any release of degraded peptide from endosomes. It has been argued that inside endosomes fluorescein may be quenched so that endosomes become invisible. Our experiments, using Alexa488-labelled R9 clearly refute this point. For this reason, the lack of endosomal fluorescence in HEK cells cannot be due to quenching of fluorescence. We were surprised ourselves by the similarity of the degree of colocalization for the fluorescein- and Alexa488-labelled peptides. This observation may be attributed to the fact that we address uptake during the first 30 min of incubation when peptides should still be located in early and sorting endosomes. Importantly, direct membrane permeation was observed for a fluorescein-labelled peptide. It had been argued before that a fluorophore interferes with this uptake route [22]. Furthermore, it had been reported that fluorescein labelled peptides may lead to misinterpretations of peptide localization due to quenching of membrane associated

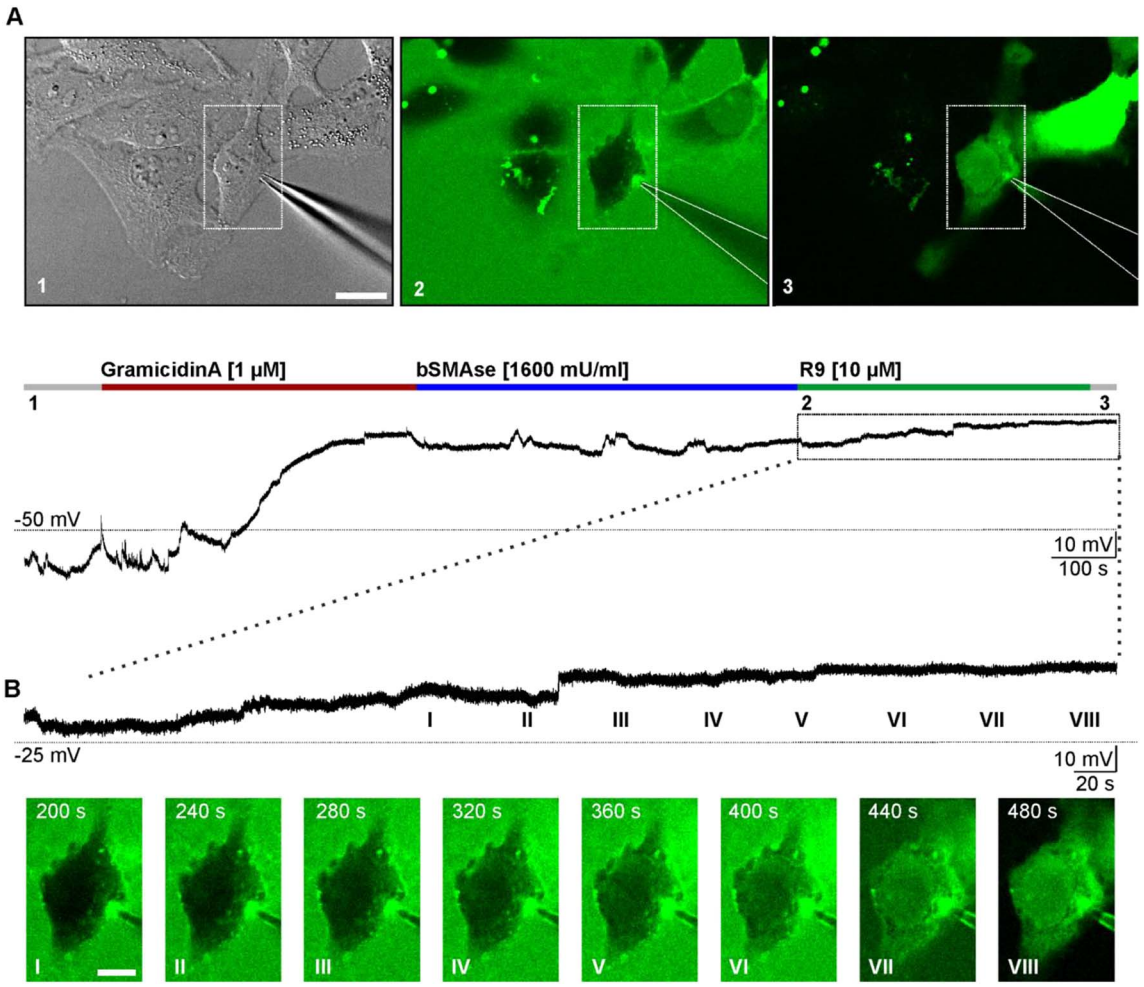

Fig. 6. Monitoring the membrane potential for the nucleation zone-dependent uptake of R9 simultaneously with confocal microscopy. (A) Representative membrane voltage (V_{mem}) recording (whole-cell, current clamp) from a HeLa cell together with exemplary images from simultaneous time-lapse confocal microscopy. Incubation with gramicidin A (red horizontal bar; 8 min, 1 μM) induces depolarization. Subsequent addition of bSMase (blue horizontal bar; 10 min, 1600 mU/mL) and incubation with fluorescein-labelled R9 (green horizontal bar; 10 μM) does not substantially affect membrane potential. Grey bars at the beginning and end of the recording indicate incubation with HEPES-buffered extracellular control solution. In fluorescence micrographs, the position of the patch pipette is indicated (lines), numbers correspond to timepoints during the electrophysiological recording. In the electrophysiological recording, the horizontal line indicates membrane potential at −50 mV. (B) Enlargement of A illustrating R9 uptake and membrane potential over time. Positions of roman numerals in the voltage trace correspond to the respective fluorescence images. Washout of fluorescein-labelled R9 (VIII) reveals the strong peptide uptake by the analyzed cell. Membrane potential at −25 mV is indicated by the horizontal line. Scale bars denote 20 μm (A) and 10 μm (B). (For interpretation of the references to colour in this figure legend, the reader is referred to the web version of this article.)

peptides [35]. We were not able to recapitulate these findings. Instead, our data demonstrated that unlabelled peptide drives the cytoplasmic uptake of fluorescently labelled peptides.

Our lipidomic analyses show that, in contrast to HeLa cells, the plasma membrane of HEK cells contains only small amounts of sphingomyelin, thus indicating that sphingomyelin is a key determinant for control of the permissiveness of the membrane towards peptide transport. Importantly, as a consequence of the scarcity of sphingomyelin in HEK cell membranes, only small amounts of ceramide can be formed. Nevertheless, conversion of these small amounts of sphingomyelin strongly increases entry kinetics and efficiency also at lower temperatures.

In line with these observations, it had been shown that the DNA methyltransferase inhibitor decitabine increases the sensitivity of drug-resistant cancer cells to chemotherapeutics by decreasing the sphingomyelin content in the plasma membrane [36]. On the other hand, it was not possible to recapitulate the differences in membrane permeation using large unilamellar vesicles formulated with/without sphingomyelin. R9 showed a good penetration that was about 30% of the one observed for the “gold standard” TP1. The relative activities of R9 and penetratin followed the same order as reported for plasma membrane-derived vesicles [37]. Instead of TP1, in this publication the hydrophobic CPP TP10 was used which showed the highest penetration. It was also demonstrated that membrane proteins play an important role in the direct membrane permeation of R9 in line with the lack of penetration in our vesicle experiments. Further research will be needed in order to understand how membrane proteins affect the membrane order in a way that enables peptide penetration.

To obtain information on the molecular processes associated with the induction of nucleation zones, we performed for the first time whole-cell patch-clamp recordings simultaneously with time-lapse confocal microscopy. Instead of studying the effect of the CPP with protocols adequate for single-channel recordings [38,39], we were interested in the impact of the peptide on the whole-cell membrane potential. These recordings revealed that in HeLa cells NZ formation coincided with a strong membrane hyperpolarisation which was absent in HEK cells. This finding was very surprising since a sudden influx of a polycation should be associated with a depolarization. Currently, the molecular basis for this hyperpolarisation is unclear. Calcium-gated potassium channels are a candidate mediator [40]. Another possibility is that hyperpolarisation is a consequence of ceramide formation [41,42]. However, the hyperpolarization induced by external addition

of sphingomyelinase was less pronounced and showed much slower kinetics than the one observed upon peptide addition (Supplemental Fig. 8). It is, however, not clear yet, whether the hyperpolarization is directly associated with sphingomyelinase activation or an independent consequence of the interaction of the peptide with the plasma membrane. Following depolarization and ceramide formation, direct membrane permeation occurred without any changes in membrane potential. The restriction of the hyperpolarization to HeLa cells indicates that a resistant membrane is a prerequisite for the peptide-induced hyperpolarization. One may conceive that the membrane potential enhances peptide accumulation at the plasma membrane which contributes to the triggering of NZ-dependent import. This hypothesis is supported by the finding that gramicidin A-induced depolarization inhibits NZ formation. The fact that depolarization affected neither the uptake route nor uptake efficiency in HEK cells demonstrates that direct translocation at low concentrations and NZ-dependent uptake are fundamentally different mechanisms. The absence of depolarization upon peptide entry in HeLa cells provides further evidence that translocation does not compromise membrane integrity. This is in line with the exclusion of propidium iodide as another measure for membrane integrity [8].

As shown before, nucleation zone-dependent uptake is restricted to arginine-rich CPPs [8]. Also following sphingomyelinase treatment, no penetration was observed for the amphipathic CPP penetratin, demonstrating that this peptide does not possess the same capacity as R9 to cross the lipid bilayer (Supplemental Fig. 9). One interesting concept in lipid research is the spontaneous formation of pores or lipid ion channels [43]. The propensity of ions to traverse such pores follows the chaotropic series, which readily provides an explanation for a nucleation zone-dependent entry being restricted to arginine-rich CPPs.

Importantly, our experiments refute the role of membrane potential in peptide uptake. Once the plasma membrane is permissive for peptide translocation, the concentration gradient is sufficient to drive import into the cytoplasm. As an alternative to gramicidin A, in some studies, V_{mem} was changed by incubating cells with a potassium-rich buffer resulting in inhibition of peptide uptake [3,19,44]. Rothbard et al. showed that inducing hyperpolarization by valinomycin increased the uptake of R8 in Jurkat cells, whereas a depolarization by gramicidin A decreased uptake [19]. While our results for gramicidin A are in line with previous data, at this point, we do not have an explanation for the discrepancies of the valinomycin experiments.

Notably, removal of the glycocalyx did not affect the uptake mechanism. In an attempt to separate the contribution of GAGs and sphingomyelin, Bechara et al. showed that sphingomyelinase treatment increased uptake more strongly for wildtype cells compared to GAG-deficient cells [45]. However, these authors solely measured the total amount of internalized peptide without determining the involved uptake mechanism, which is, in our opinion, the most important factor.

In summary, we show that for peptide entry two different states of the plasma membrane can be discriminated. A resistant state which does not permit direct membrane permeation, and a permissive state for which permeation occurs independent of membrane potential. By changing the lipid composition, notably conversion of sphingomyelin into ceramide, the resistant state can be converted into a permissive state. It will be very interesting to relate import efficiencies in vivo to sphingomyelin content and explore this concept also with regard to other types of molecular scaffolds for cytoplasmic delivery.

Acknowledgements

The authors thank Dr. Thomas Heimburg (Niels Bohr Institute, University of Copenhagen) for helpful discussions. Jürgen Schiller thanks the German Research Foundation (SFB 1052/Z3 and SCHI 476/16-1) for funding. Marc Spehr is a Lichtenberg professor of the Volkswagen foundation, R. Alis Olea received a scholarship from the Radboudumc scholarship funds. Marco J. Klein and Anne S. Ulrich thank Hoffmann-La Roche for a Postdoctoral Fellowship for MJK, and Lucie Caillon acknowledges the Fondation Ernst & Margarete Wagemann for financial support.

Appendix A. Supplementary data

Supplementary data to this article can be found online at http://dx.doi.org/10.1016/j.jconrel.2017.04.013.

References

[1] E. Koren, V.P. Torchilin, Cell-penetrating peptides: breaking through to the other side, Trends Mol. Med. 18 (2012) 385–393.
[2] C.Y. Jiao, D. Delaroche, F. Burlina, I.D. Alves, G. Chassaing, S. Sagan, Translocation and endocytosis for cell-penetrating peptide internalization, J. Biol. Chem. 284 (2009) 33957–33965.
[3] M. Kosuge, T. Takeuchi, I. Nakase, A.T. Jones, S. Futaki, Cellular internalization and distribution of arginine-rich peptides as a function of extracellular peptide concentration, serum, and plasma membrane associated proteoglycans, Bioconjug. Chem. 19 (2008) 656–664.
[4] J. Mueller, I. Kretzschmar, R. Volkmer, P. Boisguerin, Comparison of cellular uptake using 22 CPPs in 4 different cell lines, Bioconjug. Chem. 19 (2008) 2363–2374.
[5] P. Lönn, S.F. Dowdy, Cationic PTD/CPP-mediated macromolecular delivery: charging into the cell, Expert. Opin. Drug Deliv. 12 (2015) 1627–1636.
[6] W.P. Verdurmen, P.H. Bovee-Geurts, P. Wadhwani, A.S. Ulrich, M. Hallbrink, T.H. van Kuppevelt, R. Brock, Preferential uptake of L- versus D-amino acid cell-penetrating peptides in a cell type-dependent manner, Chem. Biol. 18 (2011) 1000–1010.
[7] R. Brock, The uptake of arginine-rich cell-penetrating peptides: putting the puzzle together, Bioconjug. Chem. 25 (2014) 863–868.
[8] F. Duchardt, M. Fotin-Mleczek, H. Schwarz, R. Fischer, R. Brock, A comprehensive model for the cellular uptake of cationic cell-penetrating peptides, Traffic 8 (2007) 848–866.
[9] W.P. Verdurmen, M. Thanos, I.R. Ruttekolk, E. Gulbins, R. Brock, Cationic cell-penetrating peptides induce ceramide formation via acid sphingomyelinase: implications for uptake, J. Control. Release 147 (2010) 171–179.
[10] H. Hirose, T. Takeuchi, H. Osakada, S. Pujals, S. Katayama, I. Nakase, S. Kobayashi, T. Haraguchi, S. Futaki, Transient focal membrane deformation induced by arginine-rich peptides leads to their direct penetration into cells, Mol. Ther. 20 (2012) 984–993.
[11] F. Duchardt, I.R. Ruttekolk, W.P. Verdurmen, H. Lortat-Jacob, J. Burck, H. Hufnagel, R. Fischer, H. van den M, D.W. Lowik, G.W. Vuister, A. Ulrich, W. de M, R. Brock, et al., J.Biol.Chem. 284 (2009) 36099–36108.
[12] H.C. Christianson, M. Belting, Heparan sulfate proteoglycan as a cell-surface endocytosis receptor, Matrix Biol. 35 (2014) 51–55.
[13] M.E. Favretto, R. Wallbrecher, S. Schmidt, R. van de Putte, R. Brock, Glycosaminoglycans in the cellular uptake of drug delivery vectors - bystanders or active players? J. Control. Release 180C (2014) 81–90.
[14] I. Nakase, A. Tadokoro, N. Kawabata, T. Takeuchi, H. Katoh, K. Hiramoto, M. Negishi, M. Nomizu, Y. Sugiura, S. Futaki, Interaction of arginine-rich peptides with membrane-associated proteoglycans is crucial for induction of actin organization and macropinocytosis, Biochemistry 46 (2007) 492–501.
[15] J.P. Richard, K. Melikov, H. Brooks, P. Prevot, B. Lebleu, L.V. Chernomordik, Cellular uptake of unconjugated TAT peptide involves clathrin-dependent endocytosis and heparan sulfate receptors, J. Biol. Chem. 280 (2005) 15300–15306.
[16] M. Tyagi, M. Rusnati, M. Presta, M. Giacca, Internalization of HIV-1 tat requires cell surface heparan sulfate proteoglycans, J. Biol. Chem. 276 (2001) 3254–3261.
[17] H.L. Amand, H.A. Rydberg, L.H. Fornander, P. Lincoln, B. Norden, E.K. Esbjorner, Cell surface binding and uptake of arginine- and lysine-rich penetratin peptides in absence and presence of proteoglycans, Biochim. Biophys. Acta 1818 (2012) 2669–2678.
[18] S.T. Henriques, M.A. Castanho, Consequences of nonlytic membrane perturbation to the translocation of the cell penetrating peptide pep-1 in lipidic vesicles, Biochemistry 43 (2004) 9716–9724.
[19] J.B. Rothbard, T.C. Jessop, R.S. Lewis, B.A. Murray, P.A. Wender, Role of membrane potential and hydrogen bonding in the mechanism of translocation of guanidinium-rich peptides into cells, J. Am. Chem. Soc. 126 (2004) 9506–9507.
[20] S. Schmidt, M.J. Adjobo-Hermans, R. Wallbrecher, W.P. Verdurmen, P.H. Bovee-Geurts, J. van Oostrum, F. Milletti, T. Enderle, R. Brock, Detecting cytosolic peptide delivery with the GFP complementation assay in the low micromolar range, Angew. Chem. Int. Ed. Eng. 54 (2015) 15105–15108.
[21] S. Schmidt, M.J. Adjobo-Hermans, R. Kohze, T. Enderle, R. Brock, F. Milletti, Identification of short hydrophobic cell-penetrating peptides for cytosolic peptide delivery by rational design, Bioconjug. Chem. 28 (2017) 382–389.
[22] E. Dupont, A. Prochiantz, A. Joliot, Identification of a signal peptide for unconventional secretion, J. Biol. Chem. 282 (2007) 8994–9000.
[23] J.L. Harris, B.J. Backes, F. Leonetti, S. Mahrus, J.A. Ellman, C.S. Craik, Rapid and general profiling of protease specificity by using combinatorial fluorogenic substrate libraries, Proc. Natl. Acad. Sci. U. S. A. 97 (2000) 7754–7759.
[24] S. Veitinger, T. Veitinger, S. Cainarca, D. Fluegge, C.H. Engelhardt, S. Lohmer, H. Hatt, S. Corazza, J. Spehr, E.M. Neuhaus, M. Spehr, Purinergic signalling mobilizes mitochondrial Ca(2)(+) in mouse Sertoli cells, J. Physiol. 589 (2011) 5033–5055.
[25] Y. Yao, S. Hong, H. Zhou, T. Yuan, R. Zeng, K. Liao, The differential protein and

lipid compositions of noncaveolar lipid microdomains and caveolae, Cell Res. 19 (2009) 497–506.
[26] S. Dinkla, K. Wessels, W.P. Verdurmen, C. Tomelleri, J.C. Cluitmans, J. Fransen, B. Fuchs, J. Schiller, I. Joosten, R. Brock, G.J. Bosman, Functional consequences of sphingomyelinase-induced changes in erythrocyte membrane structure, Cell Death Dis. 3 (2012) e410.
[27] J.R. Marks, J. Placone, K. Hristova, W.C. Wimley, Spontaneous membrane-translocating peptides by orthogonal high-throughput screening, J. Am. Chem. Soc. 133 (2011) 8995–9004.
[28] G. Tunnemann, R.M. Martin, S. Haupt, C. Patsch, F. Edenhofer, M.C. Cardoso, Cargo-dependent mode of uptake and bioavailability of TAT-containing proteins and peptides in living cells, FASEB J. 20 (2006) 1775–1784.
[29] G. Tunnemann, G. Ter-Avetisyan, R.M. Martin, M. Stockl, A. Herrmann, M.C. Cardoso, Live-cell analysis of cell penetration ability and toxicity of oligo-arginines, J. Pept. Sci. 14 (2008) 469–476.
[30] D. Terrone, S.L. Sang, L. Roudaia, J.R. Silvius, Penetratin and related cell-penetrating cationic peptides can translocate across lipid bilayers in the presence of a transbilayer potential, Biochemistry 42 (2003) 13787–13799.
[31] J.L. De La Vega-Beltran, C. Sanchez-Cardenas, D. Krapf, E.O. Hernandez-Gonzalez, E. Wertheimer, C.L. Trevino, P.E. Visconti, A. Darszon, Mouse sperm membrane potential hyperpolarization is necessary and sufficient to prepare sperm for the acrosome reaction, J. Biol. Chem. 287 (2012) 44384–44393.
[32] F. Di Virgilio, P.D. Lew, T. Andersson, T. Pozzan, Plasma membrane potential modulates chemotactic peptide-stimulated cytosolic free Ca2 + changes in human neutrophils, J. Biol. Chem. 262 (1987) 4574–4579.
[33] B.W. Urban, S.B. Hladky, D.A. Haydon, Ion movements in gramicidin pores. An example of single-file transport, Biochim. Biophys. Acta 602 (1980) 331–354.
[34] Y.H. Zeidan, Y.A. Hannun, Activation of acid sphingomyelinase by protein kinase Cdelta-mediated phosphorylation, J. Biol. Chem. 282 (2007) 11549–11561.
[35] J.M. Swiecicki, F. Thiebaut, M. Di Pisa, S. Gourdin-Bertin, J. Tailhades, C. Mansuy, F. Burlina, S. Chwetzoff, G. Trugnan, G. Chassaing, S. Lavielle, How to unveil self-quenched fluorophores and subsequently map the subcellular distribution of exogenous peptides, Sci. Rep. 6 (2016) 20237.
[36] S. Vijayaraghavalu, C. Peetla, S. Lu, V. Labhasetwar, Epigenetic modulation of the biophysical properties of drug-resistant cell lipids to restore drug transport and endocytic functions, Mol. Pharm. 9 (2012) 2730–2742.
[37] J. Pae, P. Saalik, L. Liivamagi, D. Lubenets, P. Arukuusk, U. Langel, M. Pooga, Translocation of cell-penetrating peptides across the plasma membrane is controlled by cholesterol and microenvironment created by membranous proteins, J. Control. Release 192 (2014) 103–113.
[38] S. Deshayes, T. Plenat, P. Charnet, G. Divita, G. Molle, F. Heitz, Formation of transmembrane ionic channels of primary amphipathic cell-penetrating peptides. Consequences on the mechanism of cell penetration, Biochim. Biophys. Acta 1758 (2006) 1846–1851.
[39] M. Pawlak, S. Stankowski, G. Schwarz, Melittin induced voltage-dependent conductance in DOPC lipid bilayers, Biochim. Biophys. Acta 1062 (1991) 94–102.
[40] K. Melikov, A. Hara, K. Yamoah, E. Zaitseva, E. Zaitsev, L.V. Chernomordik, Efficient entry of cell-penetrating peptide nona-arginine into adherent cells involves a transient increase in intracellular calcium, Biochem. J. 471 (2015) 221–230.
[41] M. Sanchez-Alavez, I.V. Tabarean, M.M. Behrens, T. Bartfai, Ceramide mediates the rapid phase of febrile response to IL-1beta, Proc. Natl. Acad. Sci. U. S. A. 103 (2006) 2904–2908.
[42] I.V. Tabarean, H. Korn, T. Bartfai, Interleukin-1beta induces hyperpolarization and modulates synaptic inhibition in preoptic and anterior hypothalamic neurons, Neuroscience 141 (2006) 1685–1695.
[43] L.D. Mosgaard, T. Heimburg, Lipid ion channels and the role of proteins, Acc. Chem. Res. 46 (2013) 2966–2976.
[44] X. Zhang, Y. Jin, M.R. Plummer, S. Pooyan, S. Gunaseelan, P.J. Sinko, Endocytosis and membrane potential are required for HeLa cell uptake of R.I.-CKTat9, a retro-inverso Tat cell penetrating peptide, Mol. Pharm. 6 (2009) 836–848.
[45] C. Bechara, M. Pallerla, F. Burlina, F. Illien, S. Cribier, S. Sagan, Massive glycosaminoglycan-dependent entry of Trp-containing cell-penetrating peptides induced by exogenous sphingomyelinase or cholesterol depletion, Cell. Mol. Life Sci. 72 (2015) 809–820.